STRENGTHENING AND REPAIR OF SELF COMPACTING CONCRETE BEAMS

تدعيم وترميم الكمرات الخرسانية ذاتية الدمك

Ashraf M. Heniegal

Assistant prof., Civil Strut. Dept., Faculty of Industrial Education, Suez Canal University, Suez, Egypt.

E-mail: ashraf_henigal@yahoo.com

ملخص:

قام الباحثون في الآونه الاخيرة بثورة في مجال تكنولوجيا الخرسانة بعد ان كانت مكبلة بالطرق التقليدية وخصوصا الخرسانة ذاتية الدمك لما تتميز به من مميزات عديدة فقام اليابانيون بتكنولوجيا جديدة في مجال الخرسانة ذاتية الدمك وما زال التواصل في تطويرها ودراستها مستمرا. تعرض هذا البحث الى تناول دراسة سلوك الكمرات الخرسانية المسلحة ذاتية الدمك المدعمة بالياف الكربون وكذلك التى تم اصلاحها بعد تعرضها للانهيار بحقن الشروخ ثم تقويتها بالياف الكربون في منطقة الشد. وفى سياق ذلك تم تصميم ثمانى خلطات مختلفة من الخرسانة ذاتية الدمك واعداد ٢٤ كمرة خرسانية مسلحة من ذات الخلطات مقاس (١٥٠*٢٠٠*١٦٠٠ مم) بطول بحر صافى ١٥٠٠ مم وتسليح رئيسى ٢ سيخ حديد عالى المقاومة قطر ١٢ مم وحديد ثانوى ٢ سيخ طرى قطر ٦ مم وكانات حديد طرى قطر ٦ مم كل ١٢٥ مم وتم تقسيم ٢٤ كمرة على النحو التالى:

- ٨ كمرات بدون تدعيم لعمل اختبار الانحناء عليها مع قياس الحمل و الترخيم حتى الانهيار
- ٨ كمرات مدعمة بطبقة واحدة من الياف الكربون بطول ١٣٠٠ مم بعرض الكمرة مع قياس الحمل و الترخيم حتى الانهيار
- ٨ كمرات كانت قد تم اختبار الانحناء عليها بدون تدعيم ثم تم حقن شروخها وتقويتها بالياف الكربون بنفس الكمرات المدعمة مع قياس الحمل والترخيم حتى الانهيار

ومن الجدير بالذكر ان الثمانى خلطات تم اعداد واحدة منها خرسانة تقليدية و٣ خلطات خرسانة ذاتية الدمك عادية الاجهاد ثم تم اعداد خلطة تمثل الخرسانة العالية المقاومة و٣ خلطات تمثل الخرسانة ذاتية الدمك عالية المقاومة

أظهرت النتائج زيادة ملحوظة فى مؤشر المرونة للكمرات الخرسانية ذاتية الدمك والعالية المقاومة ذاتية الدمك في الكمرات الغير مدعمة والمدعمة وحتى التى تم اصلاحها. كما اظهرت النتائج ايضا ان الزيادة في سعة الحمل المسبب للانهيار كان في الكمرات ذاتية الدمك والعالية المقاومة ذاتية الدمك يزيد عن الكمرات الخرسانة التقليدية و العالية المقاومة على التوالى في بعض الكمرات. واثناء قياس الحمل المسبب لاول شرخ اتضح ان الكمرات الخرسانية ذاتية الدمك والعالية المقاومة ذاتية الدمك تظهر مبكرا عن الخرسانة التقليدية والخرسانة عالية المقاومة على التوالى .

Accepted June 30, 2012

وعلى جانب اخر اظهرت النتائج أن الكمرات ذاتية الدمك وعالية المقاومة ذاتية الدمك (بدون تدعيم و المدعمة وكذلك التى تم اصلاحها) اعطت مؤشرا مبكرا للشروخ بينما اعطت ترخيما اكبر عند الانهيار عن مثيلتها الخرسانة التقليدية وعالية المقاومة على التوالى.

في سياق الحسابات الانشائية للكمرات المدعمة والغير مدعمة أظهرت النتائج الحسابية تقاربا مع الاختبارات المعملية للحمل المسبب لاول شرخ وظهر ذلك بوضوح مع الخرسانة ذاتية الدمك عالية المقاومة بينما الحمل المسبب للانهيار كان الحمل المحسوب نظريا اكثر تقاربا مع النتائج المعملية للكمرات الغير مدعمة بينما كان متقاربا الى حد ما للكمرات المدعمة. اما من ناحية اشكال الشروخ وتوزيعها اظهرت النتائج ان الكمرات المدعمة كانت موزعة أكثرانتظاما واقل انتشارا وكانت فى الخرسانة ذاتية الدمك اقل مسافة و اكثر انتشارا.

ABSTRACT:

While there is abundant research information on ordinary concrete beams strengthening or repairing with FRP, relatively little data on the behavior of self-consolidating concrete (SCC) is available. Carbon Fiber Reinforced Polymers laminates (CFRP) was investigated for strengthening and repairing SCC and high strength self compacting concrete (HSSCC) beams subjected to one midpoint load in in order to compared to beams made of normal concrete (NC) and normal high strength self compacting concrete (NHSSCC) at the same conditions respectively.

To demonstrate the concept, this paper presents results of a laboratory investigation of 24 beams (150x200x1600 mm) on the behavior of self compacting concrete strengthening and repairing with one layer of CFRP laminate and subjected to one midpoint load, including the effect of using 8 different mixes to study the effect of mix proportions on rapped CFRP beams behavior. Test results showed that the addition of CFRP laminate to the tension surface of the beams demonstrated significantly improvement in stiffness and ultimate load capacity of beams. The response of control and strengthened beams were compared and evaluated by experimental and theoretical calculations. It was observed that ductility indexes of SCC and HSSCC beams were more efficient than NC and NHSC respectively. Load carrying capacity of control, strengthening and repairing self compacting concrete beams was closed to traditional concrete beams (about 90-95%). The paper also highlighted the crack pattern of all cases of beams which indicated more distribution and smaller crack amplitude for strengthened beams with respected to the control beams.

Keywords: Self compacting concrete; Ductility index; Cracking load; Ultimate load; Load-deflection relationship

1-INTRODUCTION

The external bonding of high-strength fiber reinforced plastics (FRP) of structural concrete members has widely gained popularity in recent years, particularly in rehabilitation works and newly built structures. Earlier comprehensive experimental investigations conducted have shown that, such strengthening method has several advantages over traditional methods, due to its high stiffness-to-weight ratio, and improved durability and flexibility. Moreover, FRP are known to be less affected by corrosive environmental conditions, provide longer life, and require less maintenance. The need for rehabilitation or strengthening of bridges, buildings and other structural elements may arise, due to one or a combination of factors including construction or design defects, increased load carrying demands, change in use of structure, structural element damage, seismic upgrade, or meeting new code requirements. These factors may cause the infrastructure to be structurally inefficient, and may make the structure functionally obsolete. Before introducing fiber reinforced polymer (FRP) as a strengthening technology, one popular technique for upgrading reinforced concrete beams was the use of external epoxy-bonded steel plates [1].

Recently, FRP sheets have shown great promise as an alternative to steel plates for concrete structure repair or strengthening. Swiss researchers pioneer work on the use of FRP as a replacement for steel in plate bonding applications [2], and numerous researchers have shown that, concrete rehabilitation using FRP is a very successful application at retrofit, or to strengthen reinforced concrete members [3]. The basic concepts of using FRP for strengthening concrete structures are covered in a review article [4]. Some researches [5, 6] have shown that fiber reinforced polymer (FRP) composites for strengthening RC members, in the form of sheets, have emerged as a viable, cost effective alternative to steel plates.

In FRP-strengthened beams, failure may occur due to beam shear, flexural compression, FRP rupture, FRP de-bonding, or concrete cover ripping [7- 9]. Based on experimental results [10], the most common failure modes are de-bonding of FRP plate, or ripping of the concrete cover. These failure modes are undesirable because the FRP plate cannot be fully utilized. Premature failure modes are caused by interfacial shear and normal stress concentration at FRP cut-off points, and at flexural cracks along the beam. The end peel mode starts at the ends of the

plates and propagates inwards along the beam. Inclined and horizontal cracks form in the concrete causing it to break away from the beam, while remaining firmly attached to the plate. This mode has been investigated experimentally and analytically by many researchers [11-13]. The peeling of CFRP composite may cause a sudden and catastrophic failure of the structure. One way to prevent the premature peeling of CFRP laminates from the concrete substrate is by using end anchorage. In fact, proper anchoring systems may help CFRP laminates develop higher stresses throughout their lengths [13, 14]. It has been found [15] that, the use of end anchorage increased the flexural capacity of strengthened beams by as much as 35%, when compared to strengthened beams without anchorage. Moreover, the anchors decreased stress concentrations and increased bond strength. A number of researchers [11, 16, and 17] have claimed a need to provide mechanical anchorage at the ends of the FRP strip to prevent catastrophic brittle failure of the strengthened beam by strip detachment. End anchorage is usually provided in the form of anchor bolts or cover plates. Similar mechanical anchorages with epoxy-bonded steel plates have been recommended [18].

It has been shown recently [5, 19-23] that, external bonding of FRP to structural concrete members is an effective and simple method to increase structural capacity, e.g., in reinforced concrete columns, or reinforced concrete beams retrofitted by FRP laminates. Despite these research efforts, studies on the multi-layered and lateral faces side strips of CFRP strengthened RC beams are relatively few, especially with regard to its flexural strengthening aspect. Also, significant structural improvement was observed in terms of ultimate capacity and stiffness, although de-bonding of plates was a concern in some studies [19, 24, 25].

2-FLEXURAL STRENGTHENING

Analytical approach to evaluate the contribution of FRP composite laminates to concrete structures in flexural behavior is described in the code CEB-FIP [26]. The code uses a rectangular stress block to determine the equilibrium forces acting on the reinforced concrete beams. These codes adopt the traditional sectional analysis called "plane sections remain plane" for strain compatibility, and the stress strain relationships of concrete, steel and FRP laminates are used for equilibrium equations, Fig. (1).

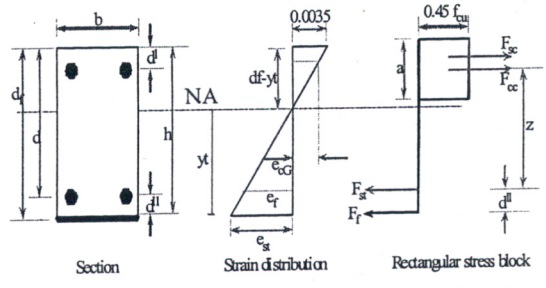

Fig.(1): Strain and stress distribution of strengthened beams with CFRP laminate.

The cracking moment Mcr of the strengthened beams may be computed as follows

$M_{cr}= f_r I_g/y_t$ (1)

Where, yt is the distance from the neutral axis to the tension face of the beam, f_r is the modulus of rupture of concrete, and I_g is the second moment of inertia of the cross section around the neutral axis. The first cracking load P_{cr} is then calculated from the cracking moment. According to the code provision CEB-FIP [26], the ultimate moment capacity of the strengthened beam is calculated using equivalent rectangular stress block of the beam cross section, and then the failure load is calculated. The total loads due to compression are equal to the total loads due to tension, as indicated in Equation (2).Taking moment at the centroid of the tension steel, A_{st} (refers to Fig. 1) and ultimate bending moment is expressed by the following equation:

$2/3\ (F_{cu} / \gamma_c)*a*b+F_{sc} = 0.45F_{cu} = F_{st}$ (2)

Getting (a), then taking moment around the centroid of tension steel, as shown in Equation (3)

$M_u = 2/3\ (F_{cu} / \gamma_c)*a*b*(d-a/2)+ F_{sc} *(d-d'')$
$= 0.45 * F_{cu} *a*b*(d-a/2)+ F_{sc} *(d-d'')$ (3)

For strengthening beams with CFRP, the total loads due to compression are equal to the total loads due to tension, as indicated in Equation (4)

$0.45Fcu*a*b+Fsc = Fst + Ff*tf$ (4)

Getting (a), then taking moment at the centroid of the tension steel for strengthening beams with CFRP as shown in Equation (5)

$Mu = 0.45Fcu * a* b* (d – a / 2) + Fsc *(d - d'') + Ff * d''$ (5)

From Mu Put can be calculated for both control (W) and strengthening beams (S). Results are shown in Table (4).

3-EXPERIMENTAL WORK

3.1-Concrete

The 28-day concrete having average compressive strength shown in Table (1), which represents the results of 8 mixes with 4 types of concrete, namely; normal concrete (M1-NC), self compacting concrete (M2-SCC1, M3-SCC2 and M4-SCC3), normal high strength concrete (M5-NHSC) and self compacting high strength concrete (M6-HSSCC1, M7-HSSCC2 and M8-HSSCC3). The concrete is prepared with the mix proportion by weight of ordinary locally available Portland cement, natural sand, and dolomite aggregate. The water-cement ratio is 0.42 for NC, (0.36-0.4) for SCC, 0.32 for NHSCC and (0.25-0.42) for HSSCC. The beams are cast from the same batch. Standard size specimens are tested in the laboratory to determine the cube's strength and modulus of rupture of concrete at 28 days.

3.2-Materials

SCC properties are strongly affected by the characteristics of materials and mix proportion. In present work, the mix design is based on a CIB method [27]. The properties of used materials are summarized as follows:

High strength steel of 12 mm diameter is used for longitudinal tension, and mild steel of 6 mm diameter is used for compression and stirrups. The yield stress of steel reinforcement is determined by performing standard tensile tests on two specimens for each bar diameter. Accordingly, the average yield stress of high strength steel is 380 MPa, and that of mild steel is 240 MPa.

Locally produced ordinary Portland cement OPC complied with E.S.S.373/91 requirements is used.

Siliceous natural sand fine aggregate passing through 4.75 mm sieve, and of specific gravity of 3.66 is applied. It is 1655 kg/m3.

The coarse aggregates are crushed dolomite with maximum nominal size 15 mm and specific gravity of 2.7. The weight of used dolomite is 1700 kg/m3.

Silica fume is a by-product of the ferrosilicon industry. It is a rich silicon dioxide powder of about 0.1 μm average size.

Viscosity Enhancing Agent (VEA), of commercial name "Sika-Viscocrete 5–400" from Sika Egypt, is used as a superplasticizer.

Carbon fiber reinforced polymer laminate CFRP is used to strengthen or to repair basic beams. MBRACE FIBER C1-30 by the BASF chemical company is used as a CFRP laminate in this research. The mechanical properties of the strengthening materials and epoxy resins, as reported by the manufacturers, are shown in Table (2). There are several constituents in commercially available SIKADU-330 of two compounds (A) and (B) used as epoxy resins.

CFRP application process on the beams is as follows:

1-The concrete substrate is checked, so that it should be free of any defects or protrusions that, could affect the ability of CFRP to bond to the concrete beams.

2-Since the beams specimens are cast in high quality smooth wood forms, the surface of the beams is extremely smooth. The concrete substrate is prepared by sandblasting, to achieve a minimum surface texture. The surface is lightly brushed using a heavy-duty scrub brush to remove any dust or loose debris after mechanical abrasion.

3-Primer is applied to the concrete surface using a small nap roller.

4-Putty is applied to the primed surface with a trowel to fill any surface defects.

5-Resin-saturated SIKADUR-330 of two compounds (A) and (B) are attached to the concrete surface of the beams, and gently pressed into the saturant. The sheets are perfectly attached to the beam.

6-A roller is used to roll in the fibers direction to facilitate impregnation and remove air bubbles.

7-A second coat of saturant is applied with a medium nap roller.

8-The FRP is allowed to cure for at least 12 hours at ambient temperature (approximately 24°C).

3.3-Specimen size and steel reinforcement details

Fig.(2) shows the reinforcement details of experimental test beams. All beam specimens are 150 × 200 mm in cross section and 1500 mm in span length on a simply supported span. All beams loaded at mid-span as illustrated in Plate (1), which shows the setup of the flexural test. Tested beams are reinforced with two 12 mm diameter bars, as tensile reinforcement at 169 mm effective depth. The longitudinal reinforcement ratio is about 0.75% of the beam cross-section.

Compression steel is reinforced with two 6 mm diameter bars, as tensile reinforcement. All beams are designed to fail in flexure according to the specification of the BS 8110-1 (1997) code of practice.

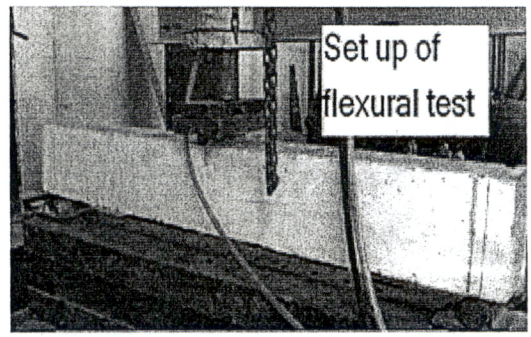

Plate (1) Setup of Flexural test

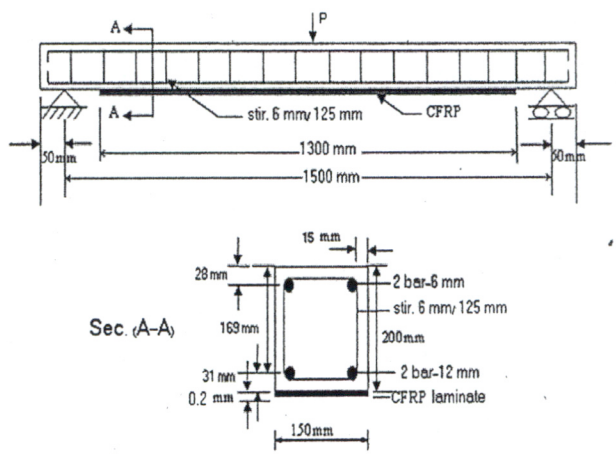

Fig. (2) longitudinal and cross section details of tested beams

3.4-Instrumentation and test procedure

Loading increases monotonically until failure of the beam. Specimens are tested at midpoint, using static loading over a 1500 mm simply supported span, to investigate the flexural performance of different mixes of NC, SCC, NHSC, and HSSCC for control (W), repairing (R) and strengthening (S) with one layer of CFRP. Under displacement control, the mid-span load is positioned by a load

cell. Plate (1) shows the overall instrumentation details of test specimens. Static load is applied at a regular interval by universal testing machine until specimen failure. During testing, the deflection of the beam is measured at mid-span and at the location of the applied load, using one midpoint deflection dial gauge of 0.01 mm accuracy.

The load at crack initiation is noted down. Also, subsequent crack patterns are marked on the beam surface, as they develop during loading from first crack appearance until failure.

4-TEST RESULTS AND DISCUSSION

4.1- Ductility characteristics

The ductility of a beam can be defined as its ability to sustain inelastic deformation without loss in load carrying capacity, prior to failure. It is usually calculated for conventional reinforced concrete structures, as a ratio of curvature, deflection, or rotation at ultimate to yielding of steel. In the case of beams strengthened with FRP laminates, there is usually no clear yield point. However, in present study, the yield point can be observed at the end of the approximately straight line of the load-deflection curve.

Ductility is an important factor for any structural element, or for the structure itself, especially in seismic regions. A ductile material is one that can undergo large strains while resisting loads. For RC members, ductility implies the ability to sustain significant inelastic deformation prior to failure. Ductility is best expressed as an index, or as a factor, through relationship at some critical stage in the performance characteristics of a structural member. Ductility index (displacement at failure divided by displacement at yield) can give an estimation of ductility.

Table (3) and Fig.(3) show the displacement ductility of tested RC beams, using CFRP laminates. An un-strengthened beam shows more displacement or ductility as compared to that of a concrete beam, strengthened or repaired with CFRP. The maximum deflection prior to final failure of the CFRP strengthened (S) and repaired beam (R) is about 13.0 and 14.55 mm, respectively, recorded for M3-SCC2. It also indicates that, S and R beams are less ductile than the control beams (W), which show a maximum deflection of 19.15 mm for M3-SCC2. The lower value of ductility index for the S and R beams indicates the lack of ductility of such beams. It is also observed that end anchored strengthened beams show more displacement or ductility as compared to other beams. However, the observed

improvement of ductility index for self compacting concrete beams (for W, R and S) depends on the pozzolanic materials added to SCC and HSSCC beams mixes.

4.1.1- Beams without CFRP (W)

Table (3) and Fig.(3) show the displacement (ductility) of tested NC and SCC beams without CFRP laminates (M1 to M4). It is observed, that SCC beam (M1 to M3) exhibits more displacement as compared to an M1-NC concrete beam. The maximum deflection prior to final failure of M1-NC beams is about 17.64 mm, and NC beams are less ductile than SCC beams (18.14-19.15 mm maximum deflection). Ductility index for NC beams is 4.57, and that of SCC beams is 4.8-5.36. High strength concrete NHSC and HSSCC (M5 to M8) beams have less displacement ductility than NC and SCC beams (M1 to M4) of maximum displacements (14.12-16.61 mm) and ductility index (3.27-4.24). Results show, also, that HSSCC beams are more ductile than NHSC beams. Displacement and ductility index of M5-NHSC are 17.64 mm and 4.57, whereas HSSCC recorded 14.12-16.61 mm and 3.55-4.24, respectively.

The improvement of ductility of both SCC and HSSCC beams may be related to the effect of pozzolanic materials of SCC mixes, which inhibits brittle failure and reveals early initial cracks, and larger displacements prior to failure.

4.1.2- Beams repaired with CFRP

Table (3) and Fig.(3) show that, repaired beams with CFRP indicate a lack of displacement and ductility than unrepaired beams M1. Displacement and ductility index are 13.5 mm and 3.21 for repaired beams, whereas 17.64 mm and 4.57 values are reported for unrepaired beams.

On the other hand, M5-NHSC repaired beams exhibit lower values of maximum

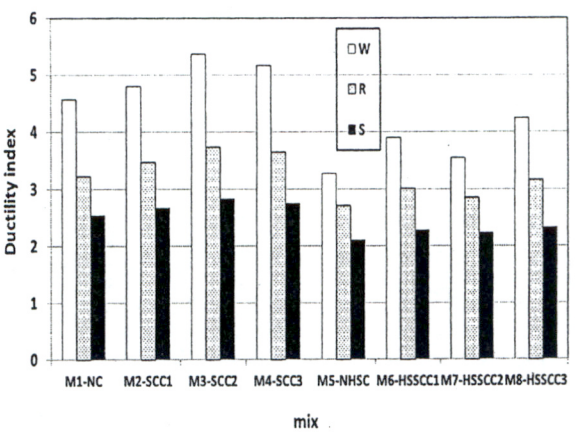

Fig. (3) Ductility index of tedted beams

deflections and ductility index than M5-NHSC unrepaired beams. Displacements and ductility index for M5-NHSC repaired beam are 12.5 mm and 2.1, whereas NHSC beams before repairing exhibit 14.11 mm and 3.27 values.

Self compacting concrete SCC repaired beams (M2 to M4) exhibit a lack of displacement and ductility index than normal concrete repaired beams M1. Displacement and ductility index are 13.5 mm and 2.54 for M1, while it is (14.2-

14.55 mm) and (2.67-2.83) for SCC beams before repairing.

However, SCC repaired beams exhibit larger displacement and ductility index than NC beams. Displacement and ductility index for SCC repaired beams are (14.2-14.55 mm) and (2.67-2.83), while they are 13.5 mm and 3.21 for repaired NC beams.

Repairing NHSC and SCHSC beams with CFRP, indicates the lack of maximum displacement and ductility index. However, HSSCC repaired beams exhibit larger maximum displacement and ductility than NHSC beams. Maximum displacement and ductility index for repaired HSSCC beams are (12.8-13.4 mm) and (2.84-3.15), while they are 12.5 mm and 3.65 for repaired NHSC beams.

Results show, also, that SCC and HSSCC beams are more ductile than NC and NHSC beams, respectively, for all control, strengthening and repairing beams. This gain of ductility could be related to the effect of silica fume of SCC mixes. Ductility index increases with silica fumes content.

4.1.3 Beams strengthened with CFRP

Results of strengthening beams with CFRP indicate less displacement and ductility index values than those of beams without CFRP. Normal concrete strengthening beam M1-NC-S deflection and ductility index are 12.68 mm and 2.1, whereas values of 17.64 mm and 4.57 are determined for beams without strengthening M1-NC-W, Table (3) and Fig. (3).

On the other hand, strengthening of NHSC beams indicates less displacement and ductility index than M1-NC-S beams. Displacement and ductility index of M5-NHSC-S are 11.55 mm and 2.1, whereas M5-NHSC-W records 14.11 mm and 3.27

Self compacting concrete SCC exhibits larger displacement and ductility index than NC strengthened with CFRP. The values are (12.8-13 mm) and (2.67-2.82) for (M2 to M4), and are 12.68 mm and 2.54 for M1, as indicated in Table (3).

HSSCC (M6 to M8) beams are improved for displacement and ductility index than M5-NHSC beams. Displacement and ductility index of NHSC beams are 11.55 mm and 2.1, and are (11.64-11.67mm) and (2.27-2.32) for HSSCC.

4.2-First cracking and ultimate loads

The first cracking load and the ultimate capacity of the strengthened and un-strengthened (without CFRP) tested beams are determined. Table (4) presents the flexural performance of theoretical and experimental values of cracking and ultimate load for tested beams. Theoretical predictions of the first cracking load is calculated from the

equivalent transformed section analysis of the beam cross-section and the ultimate load carrying capacity is predicted using equivalent stress block of the cracked cross section in accordance to the provision mentioned in BS 8110-1 (1997).

Un-strengthened (control) beam failed by yielding of steel tension reinforcement, followed by crushing of the concrete directly under mid span point bending test, when loaded in the laboratory. The control beam (M1) develops flexural tensile cracks at the point of maximum bending moment and a load of 13.31 kN. The yield load is 31.95 kN. The beam failed in flexure, due to the crushing of extreme compression zone of concrete at a load of 40.5 kN. In general, CFRP strengthened reinforced concrete beams (S), show significant increases in flexural stiffness and ultimate capacity as compared to those of control beam (W). From Table (4) and Fig.(4), the percentage increase of cracking load of M1-NC-S strengthened beams is 39%, whereas the percentage increase of ultimate load is 136%, as compared to the control beam M1-NC-W. The increase of the first crack for SCC (M2-M4) ranges between 28% and 38%, and the gain in ultimate crack is in the range132% and137%.

The results in Table (4) show, that the gain of first crack of NHSC (M5) is 41%, while that of the ultimate load is 139%. HSSCC beams (M6-M8) exhibit a range of first crack loading (46-51%) and the gain of failure load is in the range132-141%).

Results show also that, strengthening of SCC exhibits lack of first crack than NC, while it can exhibit more gain in ultimate strength depending on the mix proportion of SCC. On the other hand, HSSCC beams exhibits higher first crack loading than NHSC, and it can gain more failure load than NHSC depending on the mix proportion of HSSCC. Results show that increasing the silica fume content of SCC decreases first crack loads for all percentages, whereas it may increase the ultimate load, if silica fume content is reduced in the mix, for example M2.

Results show also, that HSSCC gains more first crack loading than NHSC for all mix proportions, whereas ultimate strength loading may increase, according to the content of silica fume. For example, M7 gains failure load, because of the reduction of silica fume content.

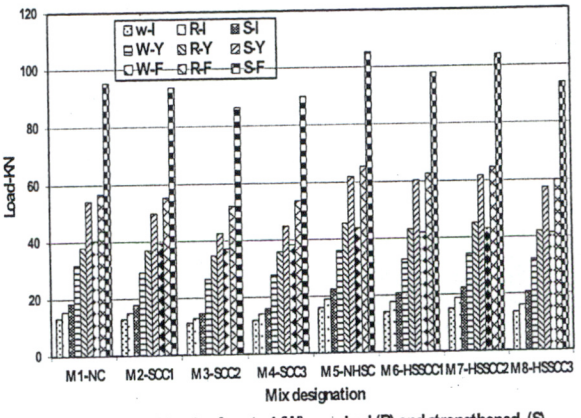

Fig. (4) Load levels of control (W), repaired (R) and strengthened (S) beams

Thus, it could be concluded that, the use of SCC influences the structural performance of strengthened beams. The ratio between calculated first cracking load and the experimentally determined value P_{cr}(th.) / P_{cr}(exp.) indicates that, the theoretical calculation gives conservative estimation of the first cracking load for control (M1-NC-W) beams (0.74), and (0.72-0.87) for SCC beams (M2-M4). But P_{cr}(th.) / P_{cr}(exp.) of the strengthened control beams (M1-NC-S) is 0.77, whereas for strengthened SCC (M2-M4) is (0.77-0.9). In general, the experimental results are in close agreement with theoretical predictions, especially for SCC.

The experimental results of P_{cr}(th.)/ P_{cr}(exp.) for NHSC is 0.91, whereas it records (0.91-1.02) for HSSCC, whereas strengthening NHSC records 0.78, and for strengthening HSSCC records (0.79-0.9). It is obvious that, HSSCC calculations are closer to experimental results than NHSC for both control and strengthening beams.

On the other hand, the ratio between theoretical and experimental ultimate load P_{ut}(th.) / P_{ut}(exp.) for control beams (W) is closer to unity (0.92-1.06), and for strengthened beams (S), the ratio is o.81 for M1-NC-W, and (0.83-0.9) for SCC beams. The ratio P_{ut}(th.) / P_{ut} (exp.) for NHSC is 0.78, while values in the range (0.79-0.86) are recorded for strengthened HSSCC beams. It is indicated, that experimental and theoretical ultimate loads are closer for all control beams, whereas for strengthening beams, SCC and HSSCC are closer in its experimental works than NC and NHSC, respectively.

4.3- Load-deflection relationship

The load-deflection behavior of the control beam and beams repaired and strengthened with CFRP laminates are shown in Figs.(4 to 6), for control (W), repaired (R), and strengthened (S) beams, respectively.

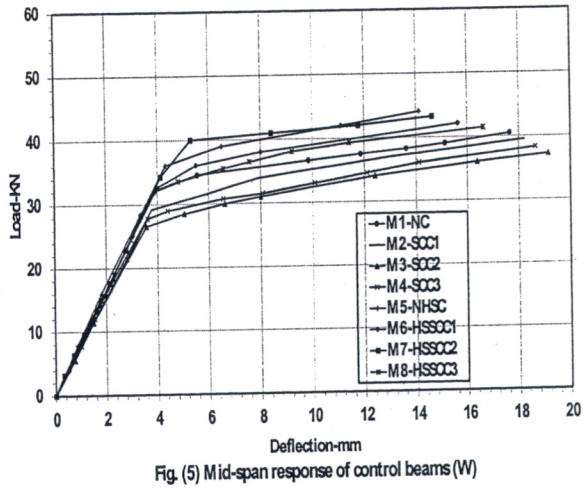

Fig. (5) Mid-span response of control beams (W)

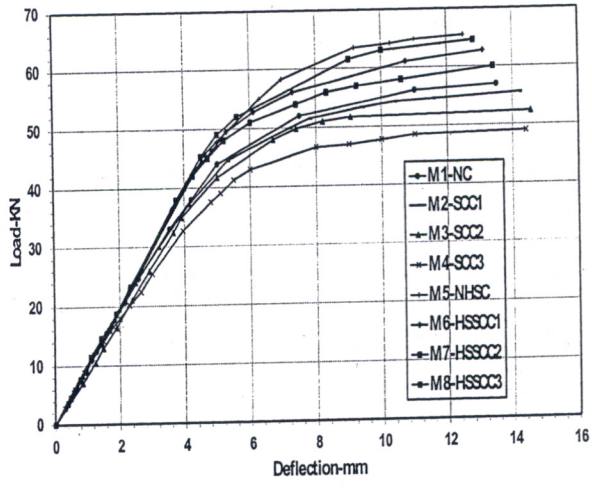

Fig. (6) Mid-span response of repaired beams (R)

4.3.1- Control beams (W)

It is observed from Fig.(4), which belongs to the control beams (W), that SCC beams (M2-M3) exhibit larger displacement than control beams. However, they exhibit smaller yielding displacement than NC beams. Besides, increasing the pozzolanic materials (silica fume) in SCC mixes exhibit more displacement and ductility as indicated in beam M3 and M4. However, capacity load of NC beams are greater than SCC beams. M1-NC has a load capacity of 40.5 KN with maximum displacement 17.6, whereas for SCC beams it ranges between (37.2-39.45 KN) with maximum displacement (18.1-19.2 mm), i.e, the reduction of load capacity is between (2.6-8) with an average of 5%, and the increase of maximum displacement is about 6%.

On the other hand, HSSCC (M6-M8) load deflection reveals the same trend of SCC (M2-M4) load-deflection relationship, but HSSCC beams are more stiffeners with higher load capacity. Maximum displacement of NHSC is 14.12 mm, while it is (14.6-17.6 mm) for HSSCC with average 14% reduction. Load capacity of NHSC (44-KN) is higher than HSSCC (41.4-43.2 KN), which has 4% average reduction.

4.3.2- Repaired beams (R)

All cracked control beams repaired with CFRP are injected with Techno-epoxy 165 (A), then the cracks are filled with a mortar of Techno grout GP and Techno bond LX, as illustrated in Plate (2).

Plate (2) Injection of cracks

Figures (4 and 5) represent the load-deflection relationship of repaired beams and load carrying capacities, which indicates more load carrying capacities than control beam and reduction of maximum displacement and ductility indexes. Beam M1-NC records an increase in load capacity by 41%, due to repairing by CFRP, while SCC beams increase by about 37%. On the other hand, the increase of load capacity of M5-NHSC records 49% and HSSCC beams record about 68%.

It is concluded, that repairing of SCC beams is closed to NC improving load capacity of repaired beams whereas, HSSCC exhibits more load capacity increments than NHSC repairing beams. It is shown from Fig. (4), also, that improvement of cracking loads of repaired beams is abut 17 % for M1-NC and 14% for SCC (M2-M4), whereas improvement of cracking load for M5-

NHSC is 19% and 18% for HSSCC beams.

4.3.3- Strengthened beams (S)

Strengthened beams exhibit more load carrying capacity than that of control beams; however, it has less maximum displacement and ductility index. Table (4) records the gain% of load capacities of strengthened beams (S) with its corresponding control beams.

The gain of load capacity is about 136 % for MI-NC, whereas it records (122-137 %) for SCC beams. On the other hand, gain of M5-NHSC beams is 139 % while HSSCC records (126-141%).

Initial crack load gain of M1-NC is 39 %, while it records (28-38 %) for SCC beams. M5-NHSC beam has a gain of initial load of 41%, while HSSCC records (46-51 %).

Fig.(7) shows that, SCC strengthened beams are less stiffener, and have larger maximum displacement than M1-NC. Results of Fig.(7) indicates, also, that M5-NHSC is more stiffener and has less maximum displacement than HSSCC beams.

4.4- Comparison between NC and SCC beams

Table (3) and Fig.(8) illustrate a comparison between M1-NC and M2-SCC1. It is shown from Fig. (8), that for W, R and S beams, both M1-NC and M2-SCC1 act the same behavior up to the load of yielding.

However, M2-SCC1 after yielding load becomes less stiffener and of larger maximum displacements for all cases of beams (W, R and S).

Maximum displacements for all cases of beams (W, R and S) for MI-NC are 17.64, 13.50, and 12.68 mm, where the maximum displacements increase for M2-SCC1 and record 18.14, 14.20 and 12.80 mm, respectively.

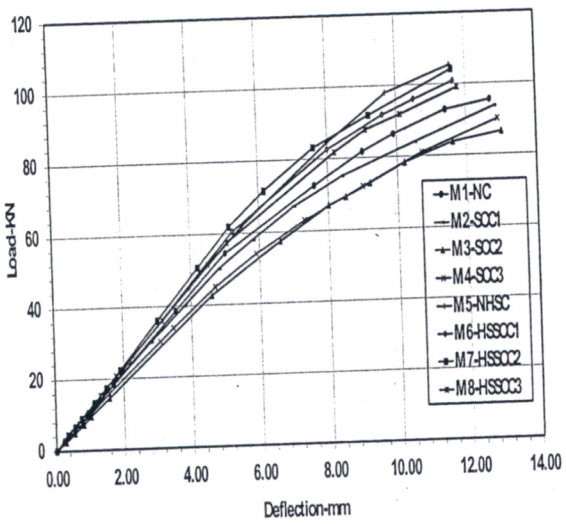

Fig. (7) Mid-span response of repaired beams (S)

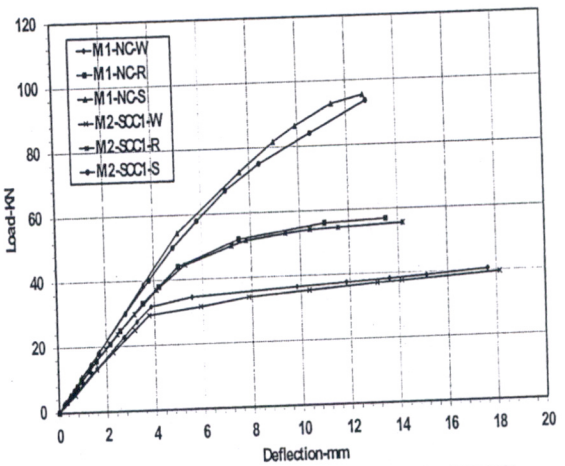

Fig. (8) Load-deflection relationship of M1-NC and M2-SCC1

Yielding loads are illustrated in Table (3), which reveals less yielding load of SCC (3.78, 4.1, and 4.8 mm) than NC (3.86, 4.2, and 5 mm) for all cases of beams (W, R and S), respectively. Hence, ductility indexes for SCC increase (4.80, 3.46 and 2.67), and for NC (4.57, 3.21 and 2.54), respectively. This suggests the increase of ductility by about 5, 8 and 5% for beam cases (W, R and S), respectively.

4.5- Comparison between NHSC and HSSCC beams

Figure (9) shows a comparison between M5-NHSC and M6-HSSCC beams for all cases (W, R and S). Results show, that SCC acts as NC up to the yielding load, hence, SCC becomes less stiffener and more maximum displacement than NC. Maximum displacement of M5-NHSC is 14.11, 12.50 and 11.55 mm for W, R and S beams, while M6-HSSCC1 records 15.62, 13.10 and 11.64 mm.

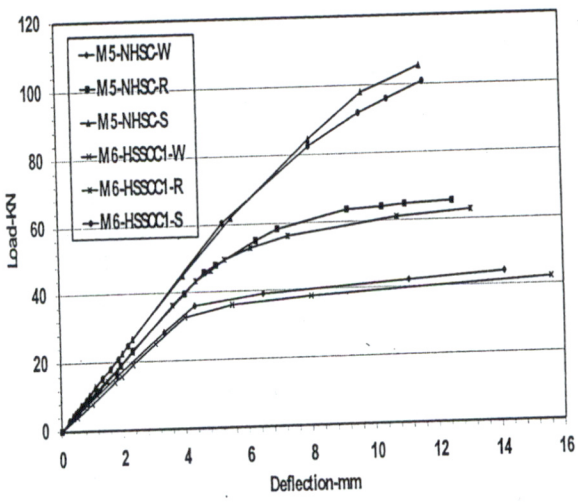

Fig. (9) Load-deflection relationship of M5-NHSC and M6-HSSCC1

Results show that yielding displacement (Δy) for HSSCC records less values than NHSC as indicated in Table (3)

Because of HSSCC have more maximum displacements and less yielding displacements, HSSCC is more ductile than of NHSC beams for all cases of beams (W, R and S).

Results of Table (3) show that yielding displacement for NHSC are 4.31, 4.63 and 5.5 mm, while HSSCC records 4, 4.36 and 5.12 mm.

Ductility index of NHSC are 3.27, 2.67 and 2.1, which are increased using HSSCC to be 3.91, 3.00 and 2.27. This means the increase in ductility index by about 20, 12, and 8 % for beam cases (W, R and S), respectively.

4.6- Crack pattern and failure modes

The failure modes which are observed on the CFRP strengthened beams are different from those of the classical control beam. The failure modes of the experimental beams are shown in Plate (3), which illustrates the failure mode of repaired beam (R) strengthened with CFRP, which indicates that new cracks are propagated to the beams (Crack 1 1nd 2), while the old repaired cracks (Crack3) still repaired without any effect. It is observed, that all beams strengthened with CFRP laminates fail in the same manner. The failure mode of specimens

with transverse edge strip is different from that of un-wrapped one.

The crack patterns and modes of failure of the control beam is illustrated in Plate (4), and for CFRP strengthened beams (S) are shown in Plates (5). During testing, the un-strengthened (control) beam exhibits widely spaced and greater number of cracks compared to the strengthened beams, especially for SCC beams.

The cracks appear on the surface of the strengthened beams at relatively close spacing of SCC and HSSCC, compared to NC and NHSC, respectively. This behavior shows the enhanced concrete confinement, due to the influence of the CFRP laminates. Also the composite action results in shifting the failure mode from flexural failure (steel yielding), in case of control beam, to peeling of CFRP laminates, for the strengthened beams. A crack normally initiates in the vertical direction, and as the load increases it extends drastically upward, due to the combined effect of shear and flexure. At higher loads, cracks propagate to top and the beam splits, i.e, in a flexure-shear failure. Finally, the beam fails due to the separation of CFRP sheet, as shown in Plate (6), giving a cracking sound along with the flexural-shear cracks.

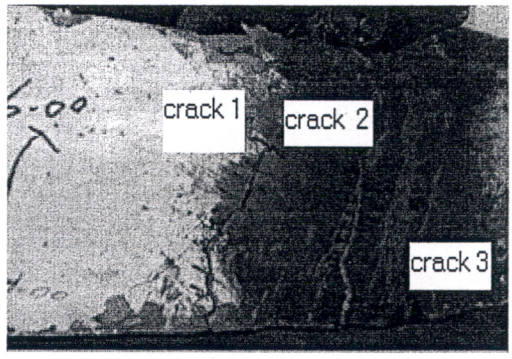

Plate (3) Mode of failure (R)

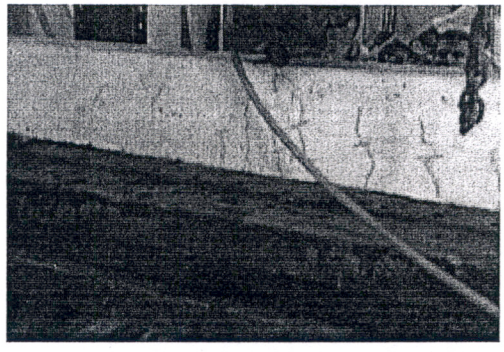

Plate (4) Mode of failure (W)

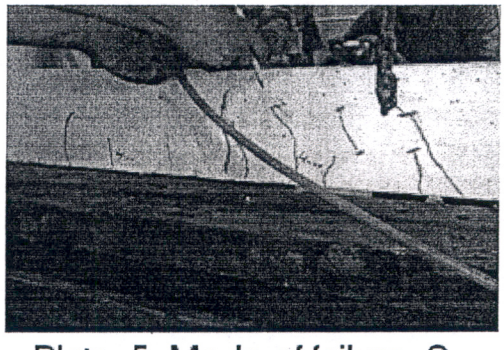

Plate (5) Mode of failure (S)

Plate (6) Separation of CFRP sheet

5-CONCLUSIONS

In this experimental investigation the flexure behavior of control (W), repaired (R) and strengthened beams (S) of NC, SCC, NHSC and HSSCC are studied. From the test results and theoretical calculations, the following conclusions are drawn:

1) The computational analysis to determine the load carrying capacity and initial cracking loads of RC beams strengthened with CFRP laminate is proved to be relatively accurate and efficient for the prediction of the experimental values of SCC and HSSCC beams.

2) Ductility indexes of SCC and HSSCC beams exhibit more values than those of NC and NHSC beams, respectively. Gain of ductility indexes of SCC beams is about 17, 11 and 16% for control, repaired, and strengthened beams, respectively, where gain of HSSCC are 30, 11 and 16%, respectively.

3) Self compacting concrete beams exhibit more maximum displacement, minor first cracking deflection, and minor yielding deflections, than traditional concrete for all cases of beams (control, repairing and strengthening).

4) Initial crack loading and load carrying capacity of both SCC and HSSCC beams appear earlier than those of NC and HSSCC beams for all cases (control, repairing and strengthening). Initial crack loading of SCC and HSSCC is about 90% NC and NHSC, respectively for all cases of beams.

5) Load carrying capacity of self compacting concrete is reduced to about 95% of traditional concrete, for all cases of beams.

6) Strengthening of RC beams with CFRP laminate increases the initial cracks loading by about 39% of NC and 28-38% of SCC beams, while load carrying capacity gain is 136% for NC and 132-137% for SCC beams. However, gain in cracking load of NHSC is 41%, while HSSCC records 46-51%, whereas gain in load carrying capacity is 139% and records 132-141% for HSSCC.

7) Repaired beams by injection of cracks and using CFRP laminate rehabilitate beams to be more stiffener and gain more load carrying capacity and more ductility indexes of SCC and HSSCC beams.

8) The crack pattern at final loads is observed from the experimental

reinforced concrete beams. Furthermore, more distribution and smaller crack amplitude are detected for strengthened beams with respected to the control beam. These effects are evident, especially for SCC strengthened beams.

6- REFERENCES

[1] Swamy, R.N., Jones, R., and Bloxham, J.W (1987), "Structural behavior of reinforced concrete beams strengthened by epoxy-bonded steel plates", Structural Engineering Part A, 65(2), pp 59-68.

[2] Meier, U., Kaiser, H (1991), "Strengthening of structures with CFRP laminates", advanced composites materials in civil engineering structures, ASCE, New York, pp 224–232.

[3] El-Badry, M (1996), "Advanced composite materials in bridges and structures", Canadian Society for Civil Engineering, Montreal.

[4] Triantafillou, T. C (1998), "Strengthening of structures with advanced FRPs", Prog. Struct. Eng. Mater, 1, pp 126– 134.

[5] Meier, U., Kaiser, H (1991), "Strengthening of structures with CFRP laminates", advanced composites materials in civil engineering structures, ASCE, New York, pp 224–232.

[6] Saadatmanesh, K., Ehsani, M.R (1991), "R/C Beam Strengthened with GFRP Plates 1: Experimental Study", Journal of Structural Engineering, pp 3434-3455.

[7] Ascione, L., Feo, L (2000), "Modeling of composite/concrete interface of RC beams strengthened with composite laminates", Composites Part B: Engineering, 31, pp 535–540.

[8] Bonacci, J.F., Maalej, M (2001), "Behavioral trends of RC beams strengthened with externally bonded FRP", Journal of Composite for Construction, 5(2), pp 102–113.

[9] Bonacci, J.F., Maalej, M (2000), "Externally bonded fiber-reinforced polymer for rehabilitation of corrosion damaged concrete beams", ACI Structural Journal, 97(5), pp 703–11.

[10] Teng, J.G. Smith, S.T., Yao, J. Chen, J.F (2003), "Intermediate crack-induced de-bonding in RC beams and slabs", Construction and Building Materials, 17,pp 447–462.

[11] Jones, R., Swamy, R.N., Charif, A (1988), "Plate separation and anchorage of reinforced concrete beams strengthened by epoxy-bonded steel plates", Struct.Eng., 66(5), pp 85–94.

[12] Saadatmanesh, H. Malek, A.M (1997), "Prediction of shear and peeling stresses at the ends of beams strengthened with FRP plates", Proc., 3rd Int. Symp. on Non-Metallic (FRP) Reinforcement for Concrete Struct., 1,

Japan Concrete Institute, Sapporo, Japan, pp 311–318.

[13] Rabinovich, O., Frostig, Y (2000), "Closed-form high-order analysis of RC beams strengthened with FRP strips", J. Compos for Constr. ASCE, 4(2), pp 65–74.

[14] Barnes, R.A. Mays, G.C (1999), "Fatigue performance of concrete beams strengthened with CFRP plates", Journal of Composites for Construction, 3(2), pp 63-72.

[15] Eshwar, N., Ibell, T., Nanni, A (2003), "CFRP strengthening of concrete bridges with curved soffits", Proceedings of International Conference on Structural Faults and Repairs, London.

[16] Garden, H.N., Hollaway, L.C (1998), "An experimental study of the influence of plate end anchorage of carbon fiber composite plates used to strengthen reinforced concrete beams", Compos. Struct, 42(2), pp 175–188.

[17] Spadea, G., Bencardino, F. and Swamy, R.N (1998), "Structural behavior of composite RC beams with externally bonded CFRP", J. Compos. Constr, 2(3), pp 132–137.

[18] Hussain, M., Sharif, A., Basunbul, I.A., Baluch, M.H., Al- Sulaimani, G.J (1995), "Flexural behavior of pre-cracked concrete beams strengthened externally by steel plates", ACI Struct. J., 92(1), pp 14–22.

[19] Alam, M.A., Zumaat, M.Z (2009), "Eliminating premature end peeling of flexurally strengthened reinforced concrete beams", Journal of applied sciences, 9(6), pp 1106-1113.

[20] Alam, M.A., Zumaat, M.Z (2009), "Eliminating premature end peeling of flexurally strengthened reinforced concrete beams", Journal of applied sciences, 9(6), pp 1106-1113.

[21] Alsayed, S.H., Al-Salloum, Y.A., Almusallam, T.H (2002), "Rehabilitation of the infrastructure using composite fabrics", final report – research project no. AR-16 52. Technical report, King Abdul Aziz City for Science and Technology (KACST), Riyadh, Saudi Arabia.

[22] Ziraba, Y.N., Baluch, M.H., Basunbul, I.A., Sharif, A.M., Azad, A.K., and Al-Sulaimani, G.J. (1994), "Guidelines toward the design of reinforced concrete beams with external plates", ACI Struct. J., 91(6), pp 639–646.

[23] Sobuz, H.R. Ahmed, E (2011), "Flexural Performance of RC Beams Strengthened with Different Reinforcement Ratios of CFRP Laminates", Key Engineering Materials, Trans Tech Publications, Vols. 471-472, pp 79-84.

[24] Aram, M.R., Czaderski, C., Motavalli, M (2008), "De-bonding

failure modes of flexural FRP-strengthened RC beams", Composites: Part B. 39, pp 826–841.

[25] Yao, J., Teng, J.G. (2007), "Plate end de-bonding in FRP-plated RC beams" I: Experiments", Engineering Structures, 29, pp 2457–471

[26] CEB-FIP, Model Code 1990, (1993), "Design Code, Comité Euro-International duBéton", Thomas Telford Services Ltd, London.

[27] Research Center for Housing, Building and Physical Planning, Cairo, Egypt. Strength of Material and Quality Control Department, "State-of-the Art-Report on Self-Compacting Concrete," October 2002.

Table (1): Mix proportion for one cubic meter

Mix	MI-NC	M2-SCC1	M3-SCC2	M4-SCC3	M5-NHSC	M6-HSSCC1	M7-HSSCC2	M8-HSSCC3
Cement (Kg)	450	450	286	238	475	450	516	320
Silica fume (Kg)	0	50	190	159	23.75	50	0	153
Sand (Kg)	730	850	882	844	493	850	816	1016
Dolomite (Kg)	1460	900	713	844	1315	925	884	687
Superplastisizer(Kg)	0	12.3	23.8	19.85	12.5	25	2.18	14.19
VEA (Kg)	0	0	0	0.4	0	0	0	0
W/C	0.42	0.36	0.39	0.4	0.32	0.25	0.42	0.37
Fcu (Kg/cm2)	445	450	450	378	700	690	700	590

Table (2): CFRP laminates and epoxy adhesive properties

Materials	Property	Values
CFRP laminate	Sheet form	Uni-directional roving
	Modulus of Elasticity (GPa)	240
	Elongation at breake (%)	1.55
	thickness (mm)	0.176
	Tensile strength (MPa)	3800
	Density (g/cm3)	1.6
	Modulus of Elasticity (GPa)	3.8
Epoxy adhesive	Elongation at break (%)	0.9
	Tensile strength (MPa)	30

Table (3): Deflections beams at yield and ultimate stages.

	Yield stage (Δy)-mm			Ultimate stage (Δu)-mm			Ductility index= (Δu)/ (Δy)		
Beam Designation	W	R	S	W	R	S	W	R	S
M1-NC	3.86	4.2	5	17.64	13.50	12.68	4.57	3.21	2.54
M2-SCC1	3.78	4.1	4.8	18.14	14.20	12.80	4.80	3.46	2.67
M3-SCC2	3.57	3.9	4.6	19.15	14.55	13.00	5.36	3.73	2.83
M4-SCC3	3.61	3.95	4.7	18.65	14.40	12.90	5.16	3.65	2.74
M5-NHSC	4.31	4.63	5.5	14.11	12.50	11.55	3.27	2.67	2.1
M6-HSSCC1	4	4.36	5.12	15.62	13.10	11.64	3.91	3.00	2.27
M7-HSSCC2	4.12	4.5	5.2	14.62	12.80	11.60	3.55	2.84	2.23
M8-HSSCC3	3.92	4.25	5.06	16.61	13.40	11.76	4.24	3.15	2.32

Table (4): Experimental and theoretical results at different load levels.

Beam Designation	Exp. Load (KN)		Theoretical load (KN)		Pcr(th)/Pcr (exp)	Put(th)/Put (exp)	Gain % due to strengthening	
	Pcr	Put	Pcr	Put			Pcr	Put
M1-NC-W	13.31	40.5	9.91	39.55	0.74	0.98	-	-
M2-SCC1-W	12.94	39.45	9.91	39.55	0.77	1.00	-	-
M3-SCC2-W	11.4	37.2	9.91	39.55	0.87	1.06	-	-
M4-SCC3-W	12	38.25	8.65	39.01	0.72	1.02	-	-
M5-NHSC-W	16	44	14.48	40.61	0.91	0.92	-	-
M6-HSSCC1-W	14.2	42.1	14.48	40.61	1.02	0.96	-	-
M7-HSSCC2-W	15	43.2	14.48	40.61	0.97	0.94	-	-
M8-HSSCC3-W	13.7	41.4	12.46	40.26	0.91	0.97	-	-
M1-NC-S	18.45	95.40	14.26	77.72	0.77	0.81	38.66	135.56
M2-SCC1-S	17.91	93.60	14.29	77.72	0.80	0.83	38.43	137.26
M3-SCC2-S	14.62	86.40	13.21	77.72	0.90	0.9	28.26	132.26
M4-SCC3-S	15.97	90.00	12.32	75.21	0.77	0.84	33.05	135.29
M5-NHSC-S	22.50	105.3	17.53	82.59	0.78	0.78	40.63	139.32
M6-HSSCC1-S	20.79	97.81	18.68	82.59	0.90	0.84	46.41	132.33
M7-HSSCC2-S	22.32	104.1	18.91	82.59	0.85	0.79	48.80	140.98
M8-HSSCC3-S	20.70	93.90	16.3	80.96	0.79	0.86	51.09	126.80